Earthquake Geotechnical Engineering for Protection and Development of Environment and Constructions – Silvestri & Moraci (Eds)
© 2019 Associazione Geotecnica Italiana, Rome, Italy, ISBN 978-0-367-14328-2

Update of the ground motion prediction equations for Italy

G. Lanzano, L. Luzi, F. Pacor, R. Puglia, C. Felicetta, M. D'Amico & S. Sgobba
Istituto Nazionale di Geofisica e Vulcanologia, Milan, Italy

ABSTRACT: The Ground Motion Prediction Equations (GMPEs) of Bindi et al. (2011) are nowadays considered as the reference predictive equations for shallow crustal events in Italy. However, the maximum usable magnitude for the hazard assessment is 6.9 and the longest periods (>1s) are not well constrained. In this paper, we discuss a new set of GMPEs for Italy: the general philosophy is to achieve the accuracy of the prediction maintaining the simplicity of the functional form used by Bindi et al (2011). We build up a dataset of Italian waveforms, adding 12 worldwide events with magnitude range 6.1 - 8.0. The dataset encompasses about 5,000 waveforms, resulting in a number of records which is about five times larger than those used by Bindi et al. (2011). The GMPEs are derived for the horizontal component of PGA, PGV and 36 ordinates of acceleration response spectra (5% damping) in the period range 0.01–10s.

1 INTRODUCTION

The Ground Motion Prediction Equations (GMPEs) estimate the median level of ground shaking and its associated uncertainty at any given site or location in given area of interest. GMPEs are essential tools in Seismic Hazard Analysis (SHA) and are commonly calibrated by regression of empirical ground motion amplitudes against a set of predictor variables, such as earthquake magnitude, source-to-site distance and local soil conditions.

The predicted median values of GMPEs are generally controlled by the choice of the functional form, adopted to simplify the complex physical process governing the ground motion. In Italy, the reference GMPEs for PSHA are those obtained by Bindi et al. (2011), named ITA10. It consists in a set of predictive equations derived from 769 records (by 150 recording stations) of 99 earthquakes in the moment magnitude range $4.1 \leq M_W \leq 6.9$, which occurred in Italy in the time span 1976-2009. However, ITA10 has some limitations: i) the maximum magnitude is 6.9 and limits the maximum usable magnitude for PSHA studies; ii) the longest period used for spectral ordinates predictions is 2s; iii) the GMPEs are available only for Joyner-Boore distance; iv) the site response is evaluated only for the Eurocode 8 (EC8) soil categories (CEN, 2003).

In order to improve and supersede ITA10, a ground motion model to predict several seismic intensity measures (IMs) in Italy (named ITA18) has been recently proposed by Lanzano et al. (2019a), including some modifications of the functional form for the median predictions and discussions on aleatory variability and epistemic uncertainty of the GMPEs. A significant improvement of ITA18 concerns the enlargement of the dataset to magnitudes larger than 6.9, to ensure a robust magnitude scaling. The large number of digital data, collected in the recent years after major seismic sequences in Italy (Emilia 2012; Central Italy 2016 - 2017), allows to extend the period range up to 10s. The availability of fault plane solutions (from Regional Centroid Moment Tensor and Centroid Moment Tensor) and 3D fault geometries, from specific literature studies, allows us to classify all the events according to their focal mechanism and calculate the distances from the rupture plane (R_{rup}), as well as the Joyner-Boore distance (R_{JB}). The extensive site characterization of strong motion station in Italy (Felicetta et al. 2017, Zimmaro et al. 2018) allows to introduce the average shear wave velocity in the uppermost 30 m, $V_{S,30}$, as explanatory variable to describe the site effects. In this paper, we briefly recall the major features of the ITA18 median model, showing some results.

2 DATASET

The dataset for GMPE calibration is composed by records included in the Engineering Strong-Motion (ESM; Luzi et al. 2016). ESM records are processed uniformly with the procedure described in Paolucci et al. (2011) and Puglia and al. (2018). The metadata and the intensity measures of ESM records are arranged in a table and disseminated through a website for the development and test of ground motion models (Lanzano et al. 2019b; esm.mi.ingv.it/flatfile-2018). It contains only records having 3 components (2 horizontal, one vertical). In this way, we are able to derive the GMPEs for horizontal and vertical components (vertical components are not discussed here) using the same dataset.

The records for GMPEs calibration are selected according to the following criteria:

- Earthquakes of active shallow crustal regions in Italy (focal depth lower than 30km);
- Minimum moment magnitude is 3.5;
- Joyner-Boore or rupture distance less than 200 km;
- Post-2009 events with magnitude less than 5.0 are characterized by revised metadata and number of records higher than 10. Several aftershocks of major seismic sequence in Italy are disregarded, in order to have, as much as possible, a homogeneous distribution of events along Italy (Figure 1a);
- Only surface instruments with low or no interactions with nearby structures are included.

We also include the records of twelve worldwide events with magnitude larger than 6.1, having a source geometry defined by specific literature studies, in order to extend the maximum usable magnitude for PSHA calculations. The maximum moment magnitude for shallow normal fault events is still 6.9 (the 1980 Irpinia earthquake), as in ITA10 and in NGA-West2 (Ancheta et al. 2014), as we could not retrieve any well documented event. Since we are aware that such events could be not representative of the regional attenuation or stress drop of Italian events, the percentage of worldwide records is small (14% of the total number of records).

We assign moment magnitudes to the events following this hierarchy: i) European-Mediterranean Earthquake Catalogue (EMEC; Grünthal, and Wahlström, 2012); ii) literature studies;

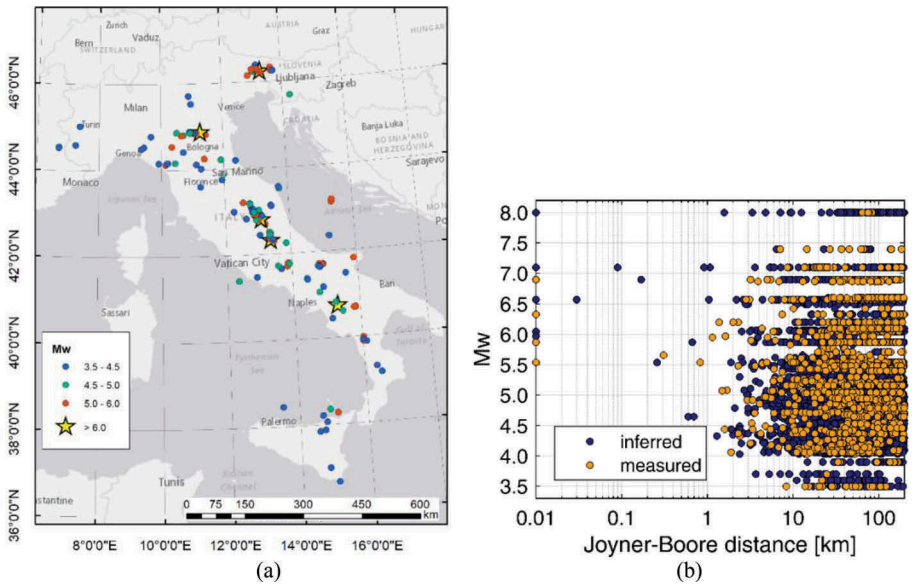

Figure 1. a) Spatial distribution of the events in Italy employed for ITA18; b) magnitude-distance distribution of the ITA18 records. Orange circles refer to stations with measured $V_{S,30}$, dark blue circles are relative to stations with $V_{S,30}$ inferred from slope (Wald and Allen, 2007).

iii) Regional Centroid Moment Tensor (Pondrelli and Salimbeni 2015) and Centroid Moment Tensor (Ekström et al., 2012); iv) Time Domain Moment Tensor (Scognamiglio et al. 2009).

The geometries of the fault ruptures are defined for the events with magnitude larger than 5.5. For smaller magnitude events, we consider point-like sources since the differences between the epicentral and Joyner-Boore distances as well as between the hypocentral and rupture distances can be neglected.

The final selection includes 5607 records, relative to 146 earthquakes and 1657 stations. Figure 1b shows the magnitude - distance distribution (Joyner-Boore distance) of the records included in the ITA18 dataset, highlighting the records of stations with $V_{S,30}$ obtained by *in-situ* measurements. About 486 stations are characterized by measured $V_{S,30}$ which corresponds to 1560 records (about 1/4 of the dataset). In case of missing $V_{S,30}$, they have been inferred from slope (Wald and Allen, 2007).

3 FUNCTIONAL FORM

ITA18 has two main differences with respect to the functional form ofBindi et al. (2011): i) a linear scaling for magnitude in the magnitude function; ii) a linear scaling with $V_{S,30}$ to describe the site effects. A summary of the functional form is:

$$\log_{10} Y = a + F_M(M_W, SOF) + F_D(M_W, R) + F_S\left(V_{S,30}\right) + \sigma \tag{1}$$

$$F_M(M_W, SOF) = f_j SOF_j + \begin{cases} b_1(M_W - M_h) \text{where} M_W \leq M_h \\ b_2(M_W - M_h) \text{where} M_W > M_h \end{cases} \tag{2}$$

$$F_D(M_W, R) = \left[c_1\left(M_W - M_{ref}\right) + c_2\right]\log_{10}\sqrt{R^2 + h^2} + c_3\sqrt{R^2 + h^2} \tag{3}$$

$$F_S\left(V_{S,30}\right) = k\log_{10}\left(\frac{V_0}{800}\right) \begin{matrix} V_0 = V_{S,30} \text{for} V_{S,30} \leq 1500 m/s \\ V_0 = 1500 m/s \text{for} V_{S,30} > 1500 m/s \end{matrix} \tag{4}$$

$$\sigma = \sqrt{\tau^2 + \varphi_{S2S}^2 + \varphi_0^2} \tag{5}$$

Y is the observed IM, i.e. the peak ground acceleration and velocity (PGA and PGV) and 36 ordinates of acceleration response spectra at 5% damping (SA) in the period (T) range 0.01–10s. The prediction is valid for RotD50, which is the median of the distribution of the Intensity Measures (IMs), obtained from the combination of the two horizontal components across all non-redundant azimuths (Boore, 2010). Since the processing is manual, high-pass filter corner frequencies may differ. As a result, the number of records varies with periods (Boore and Bommer, 2005) and reduces from 5700 at 0.1s to 4100 at 10s.

The explanatory variables are the moment magnitude M_W, the source-to-site distance R, the shear wave velocity $V_{S,30}$ and the styles of faulting SOF_j, which are dummy variables, introduced to specify strike-slip (j=1), reverse (j=2), and normal (j=3) fault types.

The hinge magnitude M_h, the reference magnitude M_{ref} and the pseudo-depth h are obtained in a first step non-linear regression. The coefficients a, b_1, b_2, c_1, c_2, c_3, k and f_j (f_1 for strike-slip, f_2 for thrust fault, and f_3 for normal fault) are derived by a second step mixed-effect linear regression (Bates et al. 2015). The random-effects are applied to stations and events, in order to estimate the partially non-ergodic sigma according to Al Atik et al (2010), where τ and ϕ_{S2S} represent between-event and site-to-site variability, respectively, and ϕ_0 is the standard deviation of the event- and site- corrected residuals. We derived two different sets of coefficients for Joyner-Boore ($R=R_{JB}$) and rupture ($R=R_{rup}$) distances and they are available in the electronic supplement of Lanzano et al. (2019a).

4 RESULTS

Figure 2 shows the observations against predictions of ITA18 and ITA10 for PGA. The comparison is carried out for 4 different combination of the explanatory variables.

The empirical data points of stiff soil sites in the top panels of Figure 2 are those recorded during the 2009 L'Aquila and 2016-2017 Central Italy seismic sequence, characterized by normal focal mechanisms. The records of the bottom panels are mainly related to the 2012 Emilia seismic sequence, occurred in the large alluvial basin of the Po river and represented by thrust faulting. ITA10 and ITA18 predicts similar strong-motion amplitudes, except for thrust fault events, for which ITA18 predicts lower values than ITA10. At intermediate-to-long periods (see Figure 3 for the ordinates of acceleration response spectra at vibration period T=1s), the predictions are very similar and the largest differences are found for large magnitudes, where ITA10 prediction are higher than ITA18. The observations at zero distance for the M_W 6.0 plots are satisfactorily included in the range of prediction of the ground motion model, with a relevant impact on seismic hazard assessment.

The anelastic attenuation term is better represented in ITA18 than ITA10, especially for normal fault events. Therefore, Luzi et al. (2017) already highlighted the poor performance of the anelastic attenuation of ITA10 against the empirical data of the 2016 Central Italy seismic sequence.

Figure 4 compares the between-event τ, within-event ϕ and total σ standard deviations of ITA10 and ITA18. We can observe a decrease of the total sigma of ITA18, w.r.t. ITA10, for periods larger than 0.1s. The larger decrease of the between-event variability is due to the improved accuracy in the location and magnitude of events, related to the growth of monitoring networks and quality of instruments. We do not observe differences in the within-event

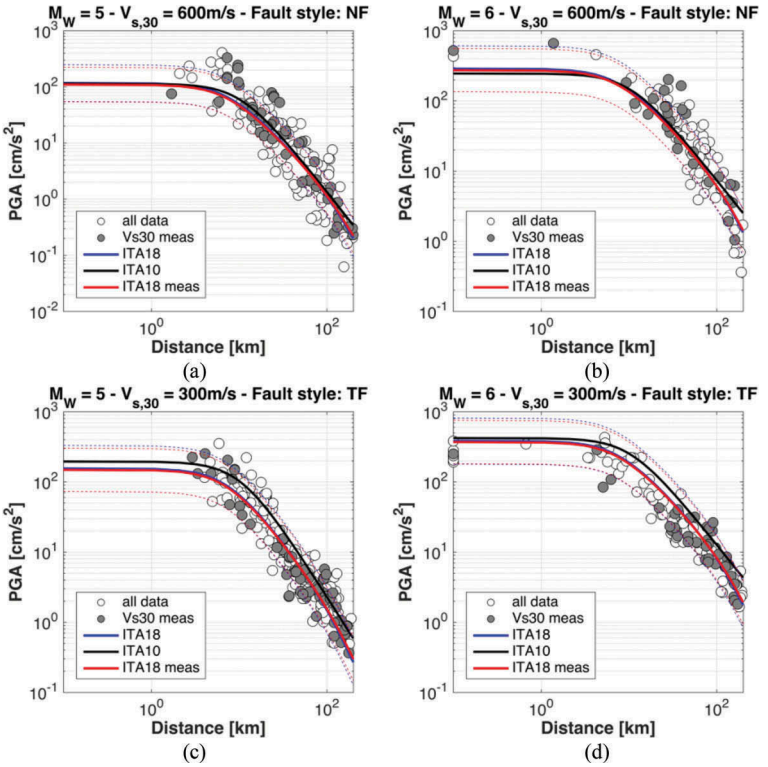

Figure 2. Predictions of ITA18, ITA18meas and ITA10 against observations for PGA: a) M_W=5.0, $V_{S,30}$ = 600 m/s and NF; b) M_W=6.0, $V_{S,30}$ = 600 m/s and NF; c) M_W=5.0, $V_{S,30}$ = 300 m/s and TF; d) M_W=6.0, $V_{S,30}$ = 300 m/s and NF. White circles are the empirical data in the range M_W±0.3 and $V_{S,30}$±100m/s; grey circles are the records of stations with measured $V_{S,30}$'s in the range M_W±0.3 and $V_{S,30}$±100m/s.

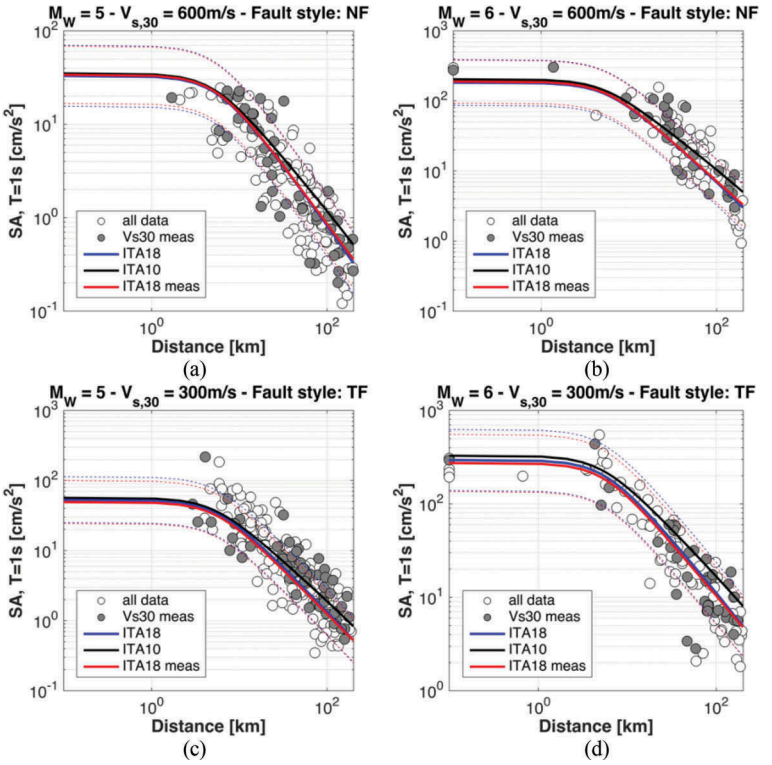

Figure 3. Predictions of ITA18, ITA18meas and ITA10 against observations for Spectral Acceleration (SA) ordinates at T=1s: a) M_W=5.0, $V_{S,30}$ = 600 m/s and NF; b) M_W=6.0, $V_{S,30}$ = 600 m/s and NF; c) M_W=5.0, $V_{S,30}$ = 300 m/s and TF; d) M_W=6.0, $V_{S,30}$ = 300 m/s and NF. White circles are the empirical data in the range $M_W \pm 0.3$ and $V_{S,30} \pm 100$m/s; grey circles are the records of stations with measured $V_{S,30}$'s in the range $M_W \pm 0.3$ and $V_{S,30} \pm 100$m/s.

standard deviation of the two models, showing a peak at 0.1s. This behavior is related to the site-to-site error (a component of within-event variability), which has the largest variability at T = 0.1s probably due to the different high frequency attenuation *kappa* among sites with the same $V_{S,30}$ (Laurendeau et al. 2013). Moreover, several stations managed by the Department of Civil Protection are installed in small masonry buildings (box), that usually host electric devices; the oscillation period of the box is very close to 0.1s (Ditommaso et al, 2010) and it could contribute to the increase of site-to-site variability.

5 INFERRED VS. MEASURED $V_{S,30}$

We investigate the impact of the use of $V_{S,30}$ inferred from proxy on GMPEs median predictions and variability. We calibrate a set of GMPEs, named ITA18meas, on a subset of records of stations with measured $V_{S,30}$ (Figure 1b), using the same functional form of ITA18.

The predictions of ITA18 and ITA18meas are similar (Figure 2), since the calibration coefficients do not significantly change. On the contrary, standard deviations are remarkably lower than ITA18 (Figure 3) and are reported in Table 1. However, the sharp peak at T=0.1s still persists.

Since the ITA18meas calibration is performed on a subset of the original dataset, the error associated to the median predictions can be larger. It can be quantified by estimating the statistical uncertainty in the predictions, calculated on the model fit and the data distribution. The epistemic uncertainty σ_μ can be calculated as (Al Atik & Youngs 2014; Bindi et al. 2017, 2019):

Table 1. Standard deviations [log10 units] of ITA18meas for some IMs.

IM	PGA	PGV	Periods of acceleration response spectra ordinates [s]						
			0.05	0.1	0.2	0.5	1.0	2.0	5.0	10.0
τ	0.137	0.133	0.144	0.153	0.146	0.137	0.152	0.148	0.136	0.118
ϕ_{S2S}	0.202	0.133	0.228	0.253	0.237	0.174	0.174	0.182	0.149	0.138
ϕ_0	0.190	0.189	0.195	0.197	0.197	0.201	0.201	0.195	0.193	0.174

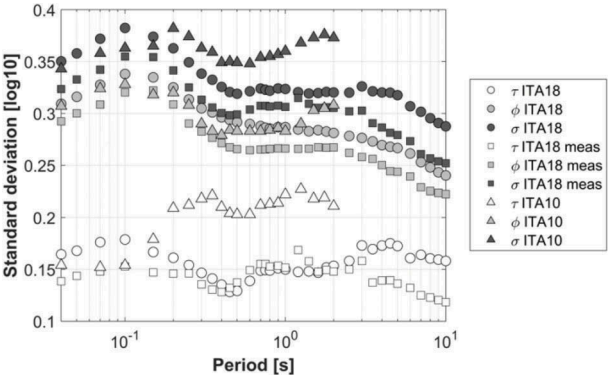

Figure 4. Standard deviations of ITA18, ITA18meas and ITA10: σ (total sigma, dark grey), τ (between-event sigma, white) and ϕ (within-event sigma, light grey).

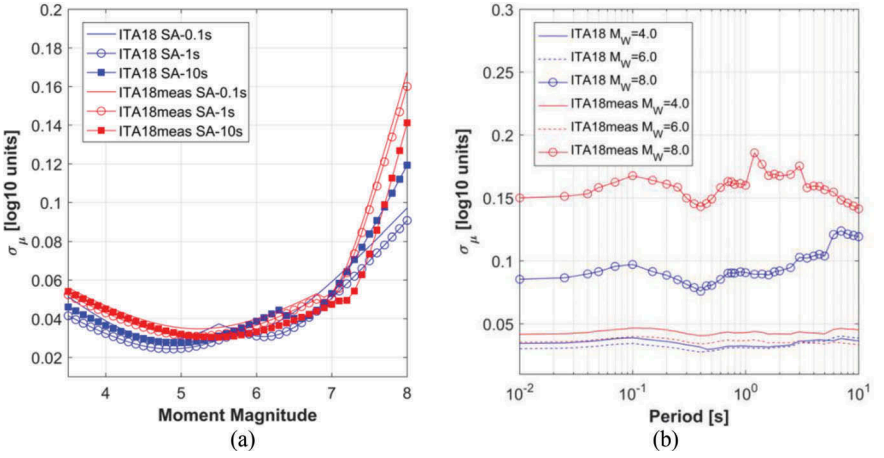

Figure 5. Epistemic uncertainty σ_μ, as a function of a) moment magnitude and b) period. σ_μ is evaluated for R_{JB}=10km, $V_{S,30}$ =300m/s and normal faulting.

$$\sigma_\mu = \sqrt{J_0^T [\mathrm{var}Cov_{x_i}] J_0} \tag{6}$$

where x_i are the data points used to develop the model, J_0 is the Jacobian matrix, i.e. the gradient of the model with respect to its coefficients, evaluated in the predictive "location" x_0, and $\mathrm{var}Cov_{xi}$ is the variance-covariance matrix of the coefficients, evaluated at all data points x_i. Since the functional forms of ITA18 and ITA18meas are the same, σ_μ quantifies the epistemic uncertainty in the median estimation solely due to the number of data used for

calibration. Figure 5 shows σ_μ as a function of magnitude and period for ITA18 and ITA18meas.

Low σ_μ values are observed in the magnitude range where the data sampling is the largest (M_W in the range 4.0 - 6.5), whereas σ_μ increases at magnitude greater than 7.0, where the data are few. No significant trend with period is observed. In general, ITA18meas exhibits σ_μ values that are similar than ITA18, except at largest magnitudes $M_W \geq 7.5$ where the error in median estimation of ITA18meas is significantly larger than ITA18.

6 CONCLUSIONS

Lanzano et al. (2019a) recalibrated the set of GMPEs for Italy, named ITA18, performing a regression on a very large dataset (5607 records, 146 events and 1657 stations), including regional and very well sampled worldwide events, in order to extend the magnitude range. The strategy for calibrating new GMPEs for Italy is to improve the predictions both in terms of median, its epistemic uncertainty and aleatory variability, while maintaining the simplicity of the functional form adopted by Bindi et al (2011).

Keeping as much data as possible, including the records from stations with $V_{S,30}$ inferred by proxies, results in a robust estimation of source scaling and attenuation with distance, but this choice causes an increase of aleatory variability, both for between-event and site-to-site variability.

In this paper, we perform an additional regression on a subset of records of stations with $V_{S,30}$ obtained by *in situ* measurement. The average reduction of standard deviations of ITA18meas with respect to ITA18 is 15% both for τ and ϕ_{S2S}. The sharp peak at SA-T=0.1s is not removed in ITA18meas, indicating that the adopted site parametrization is still not efficient in reducing the variability at this period. The error in the median prediction of ITA18meas is slightly affected by the data reduction, with the exception of Mw>7.5, for which σ_μ is higher than ITA18. As a result, the standard deviations recalibrated in this paper can be used for PSHA and other engineering applications as an alternative to those proposed by Lanzano et al. (2019a), when the $V_{S,30}$ of the investigated site has been obtained by *in-situ* measurements.

REFERENCES

Al-Atik, L., N. A. Abrahamson, J. J. Bommer, F. Scherbaum, F. Cotton, and N. Kuehn (2010). The variability of ground-motion prediction models and its components, Seismol. Res. Lett. 81(5) 794–801.

Al-Atik, L., and R. R. Youngs (2014). Epistemic Uncertainty for NGA-West2 Models, Earthq. Spectra 30(3) 1301–1318.

Ancheta, T. D., Darragh, R. B., Stewart, J. P., Seyhan, E., Silva, W. J., Chiou, B. S. J., ... & Kishida, T. (2014). NGA-West2 database. Earthquake Spectra, 30(3),989-1005.

Bates, D., M. Mächler, B. Bolker, and S. Walker (2015). Fitting linear mixed-effects models using lme4, J. Stat. Software 67 (1)1-48.

Bindi, D., F. Pacor, L. Luzi, R. Puglia, M. Massa, G. Ameri, and R. Paolucci (2011). Ground motion prediction equations derived from the Italian strong-motion database, Bull. Earthq. Eng. 9, 1899–1920.

Bindi, D., F. Cotton, S. R. Kotha, C. Bosse, D. Stromeyer, and G. Grünthal (2017). Application-driven ground motion prediction equation for seismic hazard assessments in non-cratonic moderate-seismicity areas, J. Seismol. 21(5) 1201-1218.

Bindi, D., Kotha, S. R., Weatherill, G., Lanzano, G., Luzi, L., & Cotton, F. (2019). The pan-European engineering strong motion (ESM) flatfile: consistency check via residual analysis. Bulletin of Earthquake Engineering, 17(2),583–602.

Boore, D. M., and J. J. Bommer (2005). Processing of strong-motion accelerograms: Needs, options and consequences, Soil Dynam. Earthq. Eng. 25, 93–115.

Boore, D. M. (2010). Orientation-independent, nongeometric-mean measures of seismic intensity from two horizontal components of motion. Bull. Seismol. Soc. Am. 100(4) 1830-1835.

Ditommaso, R., M. Mucciarelli, M. R. Gallipoli, and F. C. Ponzo (2010). Effect of a single vibrating building on free-field ground motion: numerical and experimental evidences, Bull. Earthq. Eng. 8(3) 693-703.

Ekström, G., M. Nettles, and A. M. Dziewonski (2012). The global CMT project 2004-2010: Centroid-moment tensors for 13,017 earthquakes, Phys. Earth Planet. Inter. 1(9) 200-201.

CEN (2003). Eurocode 8: Design of structures for earthquake resistance– Part 1: General rules seismic actions and rules for buildings, EN 1998-1, European Committee for Standardization.

Felicetta, C., M. D'Amico, G. Lanzano, R. Puglia, E. Russo, and L. Luzi (2017). Site characterization of Italian accelerometric stations, Bull. Earthq. Eng. 15(6),2329–2348.

Grünthal, G., and R. Wahlström (2012). The European-Mediterranean Earthquake Catalogue (EMEC) for the last millennium, J. Seismol. 16(3) 535–570.

Lanzano G., Luzi L., Pacor F., Felicetta C., Puglia R., Sgobba S., D'Amico M. (2019a). A revised ground motion model for shallow crustal earthquakes in Italy. Bulletin of the Seismological Society of America https://doi.org/10.1785/0120180210.

Lanzano G., S. Sgobba, L. Luzi, R. Puglia, F. Pacor, C. Felicetta, M. D'Amico, F. Cotton, and D. Bindi (2019b). The pan-European Engineering Strong-motion (ESM) flatfile: compilation criteria and data statistics, Bull. Earthq. Eng. 17(2),561–582.

Laurendeau, A., F. Cotton, O. J. Ktenidou, L. F. Bonilla, and F. Hollender (2013). Rock and stiff-soil site amplification: Dependency on VS30 and kappa (κ_0). Bull. Seismol. Soc. Am. 103(6) 3131-3148.

Luzi, L., R. Puglia, E. Russo, M. D'Amico, C. Felicetta, F. Pacor, F., G. Lanzano, U. Ceken, J. Clinton, G. Costa et al. (2016). The Engineering Strong-Motion Database: A Platform to Access Pan-European Accelerometric Data. Seismol. Res. Lett., 87(4),987–997.

Luzi, L., F. Pacor, R. Puglia, G. Lanzano, C. Felicetta, M. D'Amico, A. Michelini, L. Faenza, V. Lauciani, I. Iervolino, G. Baltzopoulos, and E. Chioccarelli (2017). The Central Italy seismic sequence between August and December 2016: analysis of strong-motion observations, Seismol. Res. Lett. 88, 1219-1231.

Paolucci, R., F. Pacor, R. Puglia, G. Ameri, C. Cauzzi, and M. Massa (2011). Record processing in ITACA, the new Italian strong-motion database, in Earthquake Data in Engineering Seismology, in Geotechnical, Geological and Earthquake Engineering Series, S. Akkar, P. Gulkan, and T. Van Eck (Editors), Vol. 14, Springer, Dordrecht, The Netherlands, 99–113.

Puglia, R., E. Russo, L. Luzi, M. D'Amico, C. Felicetta, F Pacor, and G. Lanzano (2018). Strong-motion processing service: a tool to access and analyse earthquakes strong-motion waveforms. Bull. Earthq. Eng. 16(7) 2641–2651.

Pondrelli S. and Salimbeni S., Regional Moment Tensor Review: An Example from the European Mediterranean Region. In Encyclopedia of Earthquake Engineering (pp. 1-15), http://link.springer.com/referenceworkentry/10.1007/978-3-642-36197-5_301-1, Springer Berlin Heidelberg, 2015.

Scognamiglio, L., E. Tinti and A. Michelini (2009). Real-time determination of seismic moment tensor for the Italian region. Bull. Seismol. Soc. Am. 99(4) 2223-2242.

Wald, D. J., & Allen, T. I. (2007). Topographic Slope as a Proxy for Seismic Site Conditions and Amplification. Bull. Seismol. Soc. Am. 97(5) 1379–1395.

Zimmaro, P., G. Scasserra, J.P. Stewart, T. Kishida, G. Tropeano, M. Castiglia, and P. Pelekis (2018). Strong Ground Motion Characteristics from 2016 Central Italy Earthquake Sequence, Earthq. Spectra, DOI: 10.1193/091817EQS184M.